ISSN 0915-633X

NATIONAL INSTITUTE FOR FUSION SCIENCE

Direct Energy Conversion System for D-^{3}He Fusion

Y. Tomita, L.Y. Shu and H. Momota

(Received – Oct. 16, 1993)

NIFS-252 Nov. 1993

RESEARCH REPORT
NIFS Series

NAGOYA, JAPAN

DIRECT ENERGY CONVERSION SYSTEM FOR D-^{3}He FUSION

Y.Tomita, L.Y.Shu, and H.Momota

National Institute for Fusion Science, Nagoya 464-01, Japan

[The essential part of this paper was presented at ICENES'93, Makuhari, Japan, 1993, AP-47]

KEYWORDS : D-^{3}He fueled fusion, FRC, fusion reactor, direct energy converter

DIRECT ENERGY CONVERSION SYSTEM FOR D-^{3}He FUSION

Y.Tomita, L.Y.Shu, and H.Momota

National Institute for Fusion Science, Nagoya 464-01, Japan

[The essential part of this paper was presented at ICENES'93, Makuhari, Japan, 1993, AP-47]

ABSTRACT

A novel and highly efficient direct energy conversion system is proposed for utilizing D-^{3}He fueled fusion. In order to convert kinetic energy of ions, we applied a pair of direct energy conversion systems each of which has a cusp-type DEC and a traveling wave DEC (TWDEC). In a cusp-type DEC, electrons are separated from the escaping ions at the first line-cusp and the energy of thermal ion components is converted at the second cusp DEC. The fusion protons go through the cusp-type DEC and arrive at the TWDEC, which principle is similar to "LINAC." The energy of fusion protons is recovered to electricity with an efficiency of more than 70%. These DECs bring about the high efficient fusion plant.

KEYWORDS : D-^{3}He fueled fusion, FRC, fusion reactor, direct energy converter

1. Introduction

In a D-^{3}He FRC fusion reactor such as "ARTEMIS-L," [1] more than 70% of fusion energy is carried by charged particles which escape directly out of burning plasma. By introducing these particles to direct energy converters (DEC) along the magnetic lines of force, it is expected to obtain a fusion reactor with high plant efficiency. These particles consist of thermal components with energy of few hundreds keV and fusion protons with high energy of 15 MeV. In order to convert these ion energies characterized above energy spectrum, we applied a pair of direct energy conversion systems each of which consists of a cusp-type DEC and a traveling wave DEC (TWDEC). In a cusp-type DEC, electrons are separated from the escaping ions at the first cusp and the energy of thermal ion components is converted to electricity at the second cusp. Note that the cusp-type DEC avoids unnecessary bombardment losses of energetic protons, which is inevitable to a traditional Venetian-Blind DEC [2]. The 15 MeV fusion protons pass through the cusp-type DEC without any bombardments and orbital changes because of their high energy. These protons are guided to the TWDEC and recovered their energy. The applied electric voltage in the TWDEC is less than 1MV, which is much lower than that of the flashover voltage of the insulators. In this paper, the principles of a cusp-type DEC are presented as well as a traveling wave DEC.

2. Cusp-Type Direct Energy Converter

In order to separate electrons from the escaping ions and to convert the energy of the thermal ions to electricity, we employed a double-cusp magnetic field configuration. After escaping from burning plasma, the perpendicular energy of the charged particles with respect to the magnetic field is converted to the parallel component by a reduction of magnetic field.

At the entrance of the cusp-type DEC of "ARTEMIS-L," the typical Larmor radii of electrons and thermal ions are 6×10^{-4} m and 3×10^{-2} m, respectively. Because of the small Larmor radius of electrons, they go along the constant magnetic flux surface and are introduced to the first line-cusp. The thermal ions ,which energy is characterized to be few hundreds keV, pass through the first line-cusp. The higher magnetic field at the second line-cusp compared with the first line-cusp leads the thermal ions to the second line-cusp. On the other hand, the orbit of fusion protons with energy of 15 MeV is hardly affected by this cusp-magnetic field and they pass through these line-cusps. The characteristic radius of incident fusion protons is estimated to be 2.6m in case of "ARTEMIS-L." From this incident radius, the coil radii of the inlet and outlet of the cusp-type DEC are determined to be 5.3 m and 4.2 m, respectively (Fig.1). In this case, the distances of line-cusp coils are 4.2 m and 6.4 m .

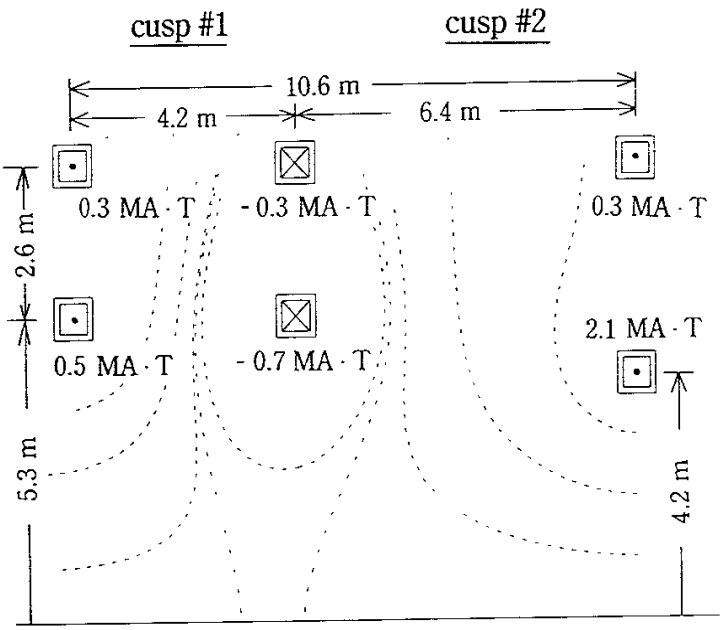

Fig.1 The arrangement of cusp type DEC ; the radii , distances and currents of cusp coils : The incident particles come from the left side. The magnetic field lines are also shown by dashed lines.

The electrons diffuse out of the burning region with the mono-energetic distribution which is characterized to be 167 keV for the plasma temperature of 83.5 keV in the "ARTEMIS - L " reactor, if the particle confinement time τ_N of ions and electrons is twice as long as the energy confinement of plasma particles τ_ε ,i.e., $\tau_N / \tau_\varepsilon = 2$. This energy corresponds to the ambipolar potential of the plasma. This potential accelerates the escaping ions out of the burning plasma. We adopt the following form as the diffused energy distribution of thermal ions :

$$f_{ion} \propto e^{-(\varepsilon-\varepsilon_{min})/\beta} \quad : \quad \varepsilon > \varepsilon_{min} \tag{1}$$

The minimum energies ε_{min} are 167 keV for proton, deuteron and triton, and 334 keV for ^{3}He and ^{4}He, respectively. The energy spread β is 167 keV for all ion species in case of $\tau_N / \tau_\varepsilon = 2$. On the other hand, fusion protons have a shifted Maxwellian energy distribution :

$$f_p \propto e^{-(\sqrt{\varepsilon}-\sqrt{\varepsilon_0})^2/\beta_p} \quad : \quad \varepsilon > \varepsilon_{min} \tag{2}$$

with the center energy ε_0 of 15 MeV and the minimum energy ε_{min} of 167 keV. The fusion reaction with a plasma temperature of about 100 keV enhances the spread of the energy distribution of fusion protons up to 1 MeV (= β_p).

The particle orbit traces bring the classification of ions with respect to their energy and the incident radius. In case that the currents of the inlet and the outlet coil are 0.8 MA · T and 2.4 MA · T (Fig.1), which high current is needed to prevent the thermal ions from passing these cusps, the particle classification diagram in ion energy and incident radius space is shown in Fig.2, where as references the characteristic radii of incident ions are also indicated. The ions with lower energy are introduced to the first line-cusp and those with higher energy pass through these cusps. The particles with middle energy bounded by two lines in

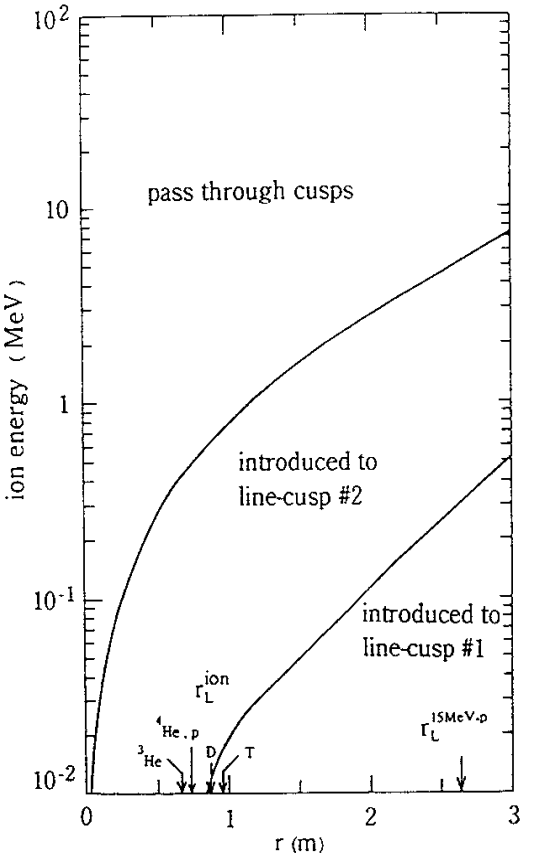

Fig.2 The particle classification diagram in ion energy and incident radius space, here as reference the characteristic incident radii of ions are also indicated.

Fig.2 are introduced to the second line-cusp or reflected to the burning region. These reflected ions will be ultimately introduced to the first line-cusp as a result of phase randomization due to the multi-periodic motion of a nonlinear oscillation. For the thermal ions whose minimum energy is 167 keV or 334 keV, lower energy parts are introduced to the second line-cusp , however higher energy parts pass through cusps. For fusion protons with incident radius of 2.6 m, the protons with higher energy than 5MeV are pass through these line-cusps (Fig.2). For the electrons , the energy scale of Fig.2 is lowered by the proton mass ratio (=1/1836). This indicates that electrons with energy of 167 keV are almost introduced to the first cusp. From the consideration of particle orbit traces included with the energy distributions, a classification fraction of incident particles is tabulated in Table 1 in case of the cusp-coil arrangement indicated in Fig.1.

Table 1 The classification fraction of incident particles to the cusp type DEC.

	electrons	thermal ions					fusion protons
		D	^{3}He	^{4}He	p	T	
introduced to line-cusp #1	> 0.99	0	0	0	0	0	0
introduced to line-cusp #2	< 0.01	0.96	0.48	0.64	0.90	1.0	< 0.01
pass through cusps	< 0.01	0.04	0.52	0.36	0.10	0	> 0.99

More than 99% of electrons are introduced to the first line-cusp. On the other hand, because of higher energy, majority of fusion protons passes through these line-cusps. A part of thermal ions is introduced to the second line-cusp, but the rest passes through these cusps. Note that higher coil-currents increase the number of thermal ions introduced to the second line-cusp but decrease the number of fusion protons to pass through these cusps. The increment of 40 % of coil-currents introduces thermal ions more than 97 % to the second line-cusp but the fraction of fusion protons to pass through decreases to 85 %. As a result, in the first line-cusp there are only electrons and in the second line-cusp there exist only thermal ions.

3. Traveling Wave Direct Energy Converter

The 15 MeV fusion protons, which pass through cusp-type DEC, are guided to the traveling wave direct energy converter [3], which consists of a modulator and a decelerator. At the modulator, a traveling electric field is excited by grid meshes

with a spacing of 1.2 m installed in the proton beams. The velocities of incident proton beams are modulated to form bunched protons at the down stream by this traveling electric field of 1 MV/m with a phase velocity of 5.3×10^7 m / s which corresponds to the velocity of 15 MeV incident protons. The applied maximum voltage to the modulator is 0.82 MV. The modulated proton beam performs a proton beam bunching at 11 m down stream from the modulator. The energy of the bunched beams is recovered by the decelerator, which utilizes a principle of a "LINAC" [4]. Namely, the bunched proton beam excites an electrostatic wave on a grid mesh array and this electrostatic field decelerates the bunched protons. By choosing the initial phase of traveling wave to be self-phasing and decelerating of incident bunched protons and controlling to match the phase velocity and the spacing of grids to the velocity of the decelerated proton beams, the energy of fusion protons is recovered to electricity with a high efficiency. The maximum voltage of 0.42 MV is applied to the decelerator. The phase trajectory of fusion protons in the traveling wave DEC is exhibited in Fig.3, where the total length of the TWDEC is 31 m and 95 % of the energy of fusion protons is decelerated.

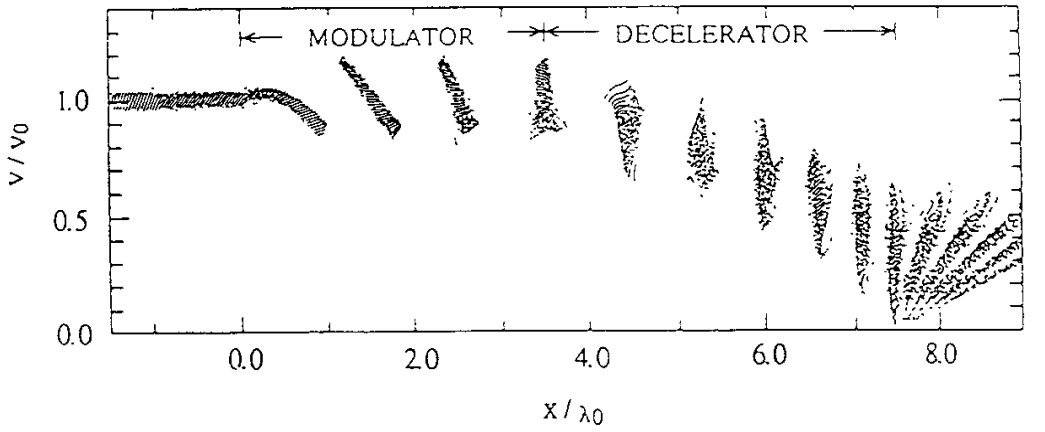

Fig.3 The phase trajectory of fusion protons in the traveling wave DEC.
The velocity is normalized by that of 15 MeV proton ($v_0 = 5.3 \times 10^7$ m/sec), and distance is measured by the wave length of 4.7 m ($= \lambda_0$) at the modulator.

The grid meshes at the modulator and the decelerator are installed with a spacing of 1.33 m. This grid pipe with 18 mm diameter and 1 mm thickness is cooled by the water with a pressure gradient of 1.2 MPa/10m. This pressure difference restrains the temperature increment at the outlet of a grid pipe to the value of 30 ℃ and the stress of grid pipes is as small as 40 MPa. Taken into consideration of bombardment of fusion protons to the grids and the energy recovery at the end collector, the conversion efficiency of the traveling wave DEC is estimated as high as 0.76 (Fig.4).

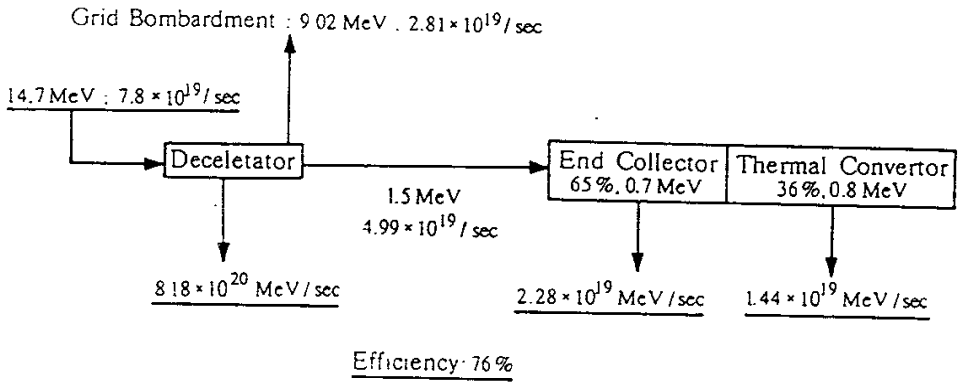

Fig. 4 The energy flow diagram of traveling wave DEC. The conversion efficiency of the traveling wave DEC is estimated as high as 0.76

4. Conclusions and Discussions

A novel and highly efficient direct energy conversion system was proposed for utilizing D-^{3}He fueled fusion reactor. It consists of a cusp-type DEC and a traveling wave DEC. In a cusp-type DEC, electrons are introduced to the first line-cusp. Thermal ions with lower energy are introduced to the second line-cusp. Concerning a higher energy part of thermal ions that pass through this cusp-type DEC, they are able to be reflected into the cusp-type DEC by use of a reflector electrode with an applied voltage of less than 1 MV, which is installed outside the outlet of the cusp-type DEC. The 15 MeV fusion protons pass almost through the cusp-type DEC, because of their high energy. This cusp-type DEC avoids completely unnecessary bombardment losses of energetic fusion protons. Thus, we confirmed a principle of the cusp-type DEC. The energy recovery of classified thermal ions is still remained as one of the future issues. Fusion protons with 15 MeV, which pass through the cusp-type DEC, are guided to a traveling wave DEC and are converted their energy to electricity with a high efficiency of more than 70%. In this TWDEC, the applied electric voltage is controlled to be less than 1 MV which allows us to avoid flashover of the insulators. The schematic drawing of the proposed DECs , i.e., the cusp-type DEC and the traveling wave DEC is given in Fig.5. By the use of these novel DECs, one is able to obtain a fusion reactor with a high plant efficiency.

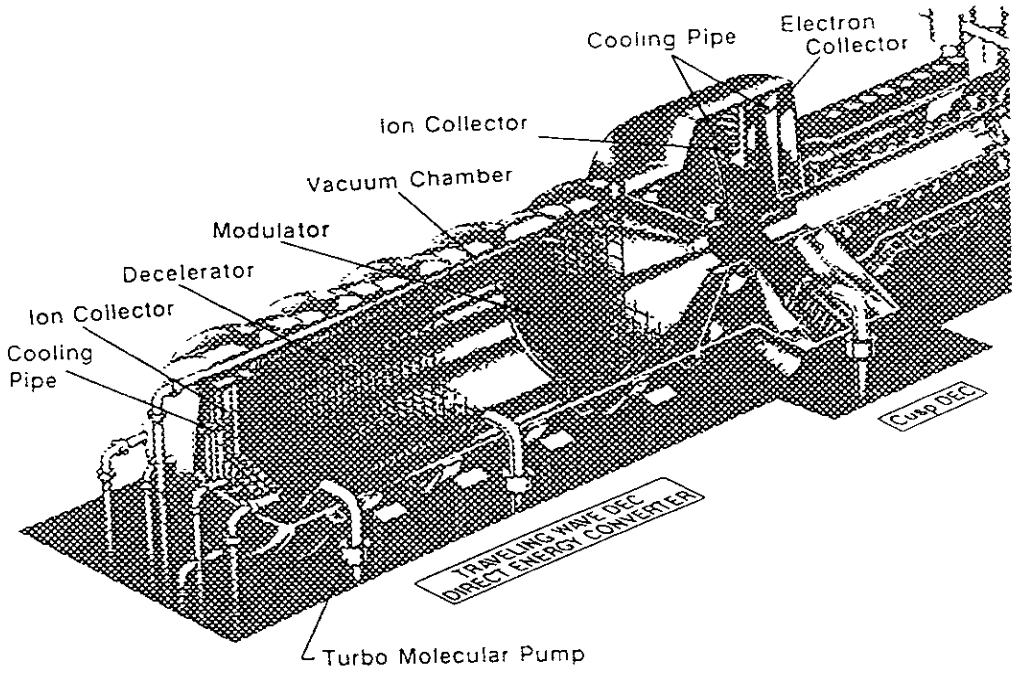

Fig.5 The schematic drawing of the proposed DECs , i.e., the cusp-type DEC and the traveling wave DEC

References

[1] H.Momota, Y.Tomita, A.Ishida, Y.Kohzaki, M.Ohnishi, S.Ohi, Y.Nakao and M.Nishikawa, "D-^{3}He Fueled FRC Reactor "ARTEMIS-L"," *Proc. 14th Int. Conf. Plasma Physics and Controlled Nuclear Fusion Research*, Wuerzburg, Germany , 1992 , IAEA, Vienna , IAEA-CN-56/G-1-13 (1992).

[2] R.W.Moir, et al., "Mirror Reactor Studies," *Proc. 6th Int. Conf. Plasma Physics and Controlled Nuclear Fusion Research*, Berchtesgaden, 1976, IAEA, Vienna, **3**, 223 (1977).

[3] H.Momota, "Direct Energy Conversion for 15 MeV Fusion Protons," LA-11808-C, Los Alamos National Laboratory , 8 (1990).

[4] D.W.Fry , R.B.R.-S.-Harvie , L.B.Mullett and W.Walkinshaw , "Travelling-Wave Linear Accelerator for Electrons," *Nature*, **160**, 351 (1947).

Recent Issues of NIFS Series

NIFS-199 M. Tanaka, *A Kinetic Simulation of Low-Frequency Electromagnetic Phenomena in Inhomogeneous Plasmas of Three-Dimensions* ; Nov. 1992

NIFS-200 K. Itoh, S.-I. Itoh, H. Sanuki and A. Fukuyama, *Roles of Electric Field on Toroidal Magnetic Confinement*, Nov. 1992

NIFS-201 G. Gnudi and T. Hatori, *Hamiltonian for the Toroidal Helical Magnetic Field Lines in the Vacuum*; Nov. 1992

NIFS-202 K. Itoh, S.-I. Itoh and A. Fukuyama, *Physics of Transport Phenomena in Magnetic Confinement Plasmas*; Dec. 1992

NIFS-203 Y. Hamada, Y. Kawasumi, H. Iguchi, A. Fujisawa, Y. Abe and M. Takahashi, *Mesh Effect in a Parallel Plate Analyzer*; Dec. 1992

NIFS-204 T. Okada and H. Tazawa, *Two-Stream Instability for a Light Ion Beam -Plasma System with External Magnetic Field;* Dec. 1992

NIFS-205 M. Osakabe, S. Itoh, Y. Gotoh, M. Sasao and J. Fujita, *A Compact Neutron Counter Telescope with Thick Radiator (Cotetra) for Fusion Experiment*; Jan. 1993

NIFS-206 T. Yabe and F. Xiao, *Tracking Sharp Interface of Two Fluids by the CIP (Cubic-Interpolated Propagation) Scheme*, Jan. 1993

NIFS-207 A. Kageyama, K. Watanabe and T. Sato, *Simulation Study of MHD Dynamo : Convection in a Rotating Spherical Shell*; Feb. 1993

NIFS-208 M. Okamoto and S. Murakami, *Plasma Heating in Toroidal Systems*; Feb. 1993

NIFS-209 K. Masai, *Density Dependence of Line Intensities and Application to Plasma Diagnostics*; Feb. 1993

NIFS-210 K. Ohkubo, M. Hosokawa, S. Kubo, M. Sato, Y. Takita and T. Kuroda, *R&D of Transmission Lines for ECH System* ; Feb. 1993

NIFS-211 A. A. Shishkin, K. Y. Watanabe, K. Yamazaki, O. Motojima, D. L. Grekov, M. S. Smirnova and A. V. Zolotukhin, *Some Features of Particle Orbit Behavior in LHD Configurations*; Mar. 1993

NIFS-212 Y. Kondoh, Y. Hosaka and J.-L. Liang, *Demonstration for Novel Self-organization Theory by Three-Dimensional Magnetohydrodynamic Simulation*; Mar. 1993

NIFS-213 K. Itoh, H. Sanuki and S.-I. Itoh, *Thermal and Electric Oscillation Driven by Orbit Loss in Helical Systems*; Mar. 1993

NIFS-214 T. Yamagishi, *Effect of Continuous Eigenvalue Spectrum on Plasma Transport in Toroidal Systems*; Mar. 1993

NIFS-215 K. Ida, K. Itoh, S.-I.Itoh, Y. Miura, JFT-2M Group and A. Fukuyama, *Thickness of the Layer of Strong Radial Electric Field in JFT-2M H-mode Plasmas*; Apr. 1993

NIFS-216 M. Yagi, K. Itoh, S.-I. Itoh, A. Fukuyama and M. Azumi, *Analysis of Current Diffusive Ballooning Mode*; Apr. 1993

NIFS-217 J. Guasp, K. Yamazaki and O. Motojima, *Particle Orbit Analysis for LHD Helical Axis Configurations* ; Apr. 1993

NIFS-218 T. Yabe, T. Ito and M. Okazaki, *Holography Machine HORN-1 for Computer-aided Retrieve of Virtual Three-dimensional Image* ; Apr. 1993

NIFS-219 K. Itoh, S.-I. Itoh, A. Fukuyama, M. Yagi and M. Azumi, *Self-sustained Turbulence and L-Mode Confinement in Toroidal Plasmas* ; Apr. 1993

NIFS-220 T. Watari, R. Kumazawa, T. Mutoh, T. Seki, K. Nishimura and F. Shimpo, *Applications of Non-resonant RF Forces to Improvement of Tokamak Reactor Performances Part I: Application of Ponderomotive Force* ; May 1993

NIFS-221 S.-I. Itoh, K. Itoh, and A. Fukuyama, *ELMy-H mode as Limit Cycle and Transient Responses of H-modes in Tokamaks* ; May 1993

NIFS-222 H. Hojo, M. Inutake, M. Ichimura, R. Katsumata and T. Watanabe, *Interchange Stability Criteria for Anisotropic Central-Cell Plasmas in the Tandem Mirror GAMMA 10 ;* May 1993

NIFS-223 K. Itoh, S.-I. Itoh, M. Yagi, A. Fukuyama and M. Azumi, *Theory of Pseudo-Classical Confinement and Transmutation to L-Mode;* May 1993

NIFS-224 M. Tanaka, *HIDENEK: An Implicit Particle Simulation of Kinetic-MHD Phenomena in Three-Dimensional Plasmas;* May 1993

NIFS-225 H. Hojo and T. Hatori, *Bounce Resonance Heating and Transport in a Magnetic Mirror;* May 1993

NIFS-226 S.-I. Iton, K. Itoh, A. Fukuyama, M. Yagi, *Theory of Anomalous Transport in H-Mode Plasmas;* May 1993

NIFS-227 T. Yamagishi, *Anomalous Cross Field Flux in CHS ;* May 1993

NIFS-228 Y. Ohkouchi, S. Sasaki, S. Takamura, T. Kato, *Effective Emission and Ionization Rate Coefficients of Atomic Carbons in Plasmas;* June 1993

NIFS-229 K. Itoh, M. Yagi, A. Fukuyama, S.-I. Itoh and M. Azumi, *Comment on 'A Mean Field Ohm's Law for Collisionless Plasmas;* June 1993

NIFS-230 H. Idei, K. Ida, H. Sanuki, H. Yamada, H. Iguchi, S. Kubo, R. Akiyama, H. Arimoto, M. Fujiwara, M. Hosokawa, K. Matsuoka, S. Morita, K. Nishimura, K. Ohkubo, S. Okamura, S. Sakakibara, C. Takahashi, Y. Takita, K. Tsumori and I. Yamada, *Transition of Radial Electric Field by Electron Cyclotron Heating in Stellarator Plasmas;* June 1993

NIFS-231 H.J. Gardner and K. Ichiguchi, *Free-Boundary Equilibrium Studies for the Large Helical Device,* June 1993

NIFS-232 K. Itoh, S.-I. Itoh, A. Fukuyama, H. Sanuki and M. Yagi, *Confinement Improvement in H-Mode-Like Plasmas in Helical Systems.* June 1993

NIFS-233 R. Horiuchi and T. Sato, *Collisionless Driven Magnetic Reconnection,* June 1993

NIFS-234 K. Itoh, S.-I. Itoh, A. Fukuyama, M. Yagi and M. *Azumi, Prandtl Number of Toroidal Plasmas;* June 1993

NIFS-235 S. Kawata, S. Kato and S. Kiyokawa , *Screening Constants for Plasma:* June 1993

NIFS-236 A. Fujisawa and Y. Hamada, *Theoretical Study of Cylindrical Energy Analyzers for MeV Range Heavy Ion Beam Probes;* July 1993

NIFS-237 N. Ohyabu, A. Sagara, T. Ono, T. Kawamura and O. Motojima, *Carbon Sheet Pumping;* July 1993

NIFS-238 K. Watanabe, T. Sato and Y. Nakayama, *Q-profile Flattening due to Nonlinear Development of Resistive Kink Mode and Ensuing Fast Crash in Sawtooth Oscillations;* July 1993

NIFS-239 N. Ohyabu, T. Watanabe, Hantao Ji, H. Akao, T. Ono, T. Kawamura, K. Yamazaki, K. Akaishi, N. Inoue. A. Komori, Y. Kubota, N. Noda, A. Sagara, H. Suzuki, O. Motojima, M. Fujiwara, A. Iiyoshi, *LHD Helical Divertor;* July 1993

NIFS-240 Y. Miura, F. Okano, N. Suzuki, M. Mori, K. Hoshino, H. Maeda. T. Takizuka, JFT-2M Group, K. Itoh and S.-I. Itoh, *Ion Heat Pulse*

after Sawtooth Crash in the JFT-2M Tokamak; Aug. 1993

NIFS-241 K. Ida, Y.Miura, T. Matsuda, K. Itoh and JFT-2M Group, *Observation of non Diffusive Term of Toroidal Momentum Transport in the JFT-2M Tokamak;* Aug. 1993

NIFS-242 O.J.W.F. Kardaun, S.-I. Itoh, K. Itoh and J.W.P.F. Kardaun, *Discriminant Analysis to Predict the Occurrence of ELMS in H-Mode Discharges;* Aug. 1993

NIFS-243 K. Itoh, S.-I. Itoh, A. Fukuyama, *Modelling of Transport Phenomena;* Sep. 1993

NIFS-244 J. Todoroki. *Averaged Resistive MHD Equations;* Sep. 1993

NIFS-245 M. Tanaka, *The Origin of Collisionless Dissipation in Magnetic Reconnection;* Sep. 1993

NIFS-246 M. Yagi, K. Itoh, S.-I. Itoh, A. Fukuyama and M. Azumi, *Current Diffusive Ballooning Mode in Seecond Stability Region of Tokamaks;* Sep. 1993

NIFS-247 T. Yamagishi, *Trapped Electron Instabilities due to Electron Temperature Gradient and Anomalous Transport;* Oct. 1993

NIFS-248 Y. Kondoh, *Attractors of Dissipative Structure in Three Disspative Fluids;* Oct. 1993

NIFS-249 S. Murakami, M. Okamoto, N. Nakajima, M. Ohnishi, H. Okada, *Monte Carlo Simulation Study of the ICRF Minority Heating in the Large Helical Device;* Oct. 1993

NIFS-250 A. Iiyoshi, H. Momota, O. Motojima, M. Okamoto, S. Sudo, Y. Tomita, S. Yamaguchi, M. Ohnishi, M. Onozuka, C. Uenosono, *Innovative Energy Production in Fusion Reactors;* Oct. 1993

NIFS-251 H. Momota, O. Motojima, M. Okamoto, S. Sudo, Y. Tomita, S. Yamaguchi, A. Iiyoshi, M. Onozuka, M. Ohnishi, C. Uenosono, *Characteristics of D-^{3}He Fueled FRC Reactor; ARTEMIS-L,* Nov. 1993